European Journal of Radiology 119 (2019) 108620

Contents lists available at ScienceDirect

European Journal of Radiology

journal homepage: www.elsevier.com/locate/ejrad

Early identification of neonatal mild hypoxic-ischemic encephalopathy by amide proton transfer magnetic resonance imaging: A pilot study

Sijin Chen[a,b], Xilong Liu[a], Yingjie Mei[c], Caixia Li[a], Daokun Ren[a], Mei Zhong[b], Yikai Xu[a,*]

[a] Department of Medical Imaging Center, Nanfang Hospital, Southern Medical University, Guangzhou 510515, China
[b] Department of Obstetrics and Gynecology, Nanfang Hospital, Southern Medical University Guangzhou 510515, China
[c] Philips Healthcare, Guangzhou, Guangdong 510055, China

ARTICLE INFO

Keywords:
APT imaging
Neonatal
Mild
Hypoxic-ischemic encephalopathy

ABSTRACT

Purpose: This study aimed to evaluate the amide proton transfer (APT) values in neonates with mild hypoxic-ischemic encephalopathy (HIE) using APT imaging.

Method: A total of 30 full-term neonates with mild HIE (16 males and 14 females; mean postnatal age 4.2 days, age range 2–7 days) and 12 normal neonates (six males and six females; mean postnatal age 3.3 days, age range 2–5 days) underwent conventional magnetic resonance imaging and APT imaging. APT measurements were performed in multiple regions of interest (ROIs) in the brain. APT values were statistically analyzed to assess for significant differences between the mild HIE and normal neonates in different regions of the brain, and correlation with neonatal gestational age.

Results: In 30 neonates with mild HIE, 10% (3/30) of the HIE patients had normal conventional MRI. There were significant differences in APT values of the HIE group in bilateral caudate, bilateral thalamus, bilateral centrum semiovale and left globus pallidus/putamen ($p < 0.05$), and no statistical difference was observed in right globus pallidus/putamen ($p = 0.051$) and brainstem ($p = 0.073$) between the two groups. Furthermore, APT values in bilateral caudate, bilateral globus pallidus/putamen, bilateral thalamus, and brainstem regions ($p < 0.05$) exhibited positive linear correlations with gestational age in the control group, except for bilateral centrum semiovale (right: Pearson's $r = 0.554$, $p = 0.062$; left: Pearson's $r = 0.561$, $p = 0.058$). In the mild HIE groups, no significant correlation with gestational age was found in all regions.

Conclusions: APT imaging is a feasible and useful technique with diagnostic capability for neonatal HIE.

1. Introduction

Neonatal hypoxic-ischemic encephalopathy (HIE) is a major complication of perinatal asphyxia, with high mortality and morbidity, and occurs in 1–6 per 1000 live births [1,2]. Neonatal HIE results in adverse neurodevelopmental outcomes, such as cerebral palsy, mental retardation and epilepsy [3]. The underlying pathophysiological mechanisms in HIE are inadequate blood flow and oxygen supply to the brain resulting in focal or diffuse brain injury. Infants with mild HIE were previously considered to have a good prognosis, without long-term disability. Therefore, there has been very limited published MRI data on neonatal mild HIE cases. However, there is increasing evidence that abnormal outcomes (such as death, and motor or developmental delay at 18 months follow-up) occur in some infants with mild HIE [4,5]. Timely diagnostic and prognostic information for mild HIE is critical, as this can aid in determining the appropriate level of treatment, can use to counsel parents, and to evaluate the effect of neuroprotective therapies.

Conventional magnetic resonance imaging has been widely used in neonatal HIE. It can help in identification and characterization of the exact location, extent, and severity of the brain injury. Newer imaging techniques have a potential role in early diagnosis and timely intervention. For example, diffusion-weighted imaging (DWI) can detect changes in the diffusion capacity of microscopic motion of water molecules. It is sensitive to early hypoxic-ischemic brain injury [6]. Magnetic resonance spectroscopy (MRS) is capable of detecting changes in concentration of metabolites in *vivo* [7], and can be used as a read out of metabolic activity which is in turn linked with metabolic function. For instance, Lactate/N-acetyl-aspartic acid (Lac/NAA) level was considered the most accurate MR biomarker. Increase in Lac concentration is an indication of increased anaerobic metabolism. The NAA level decreases in neuronal necrosis [8]. Furthermore, diffusion tensor

* Corresponding author.
E-mail address: yikaixu917@gmail.com (Y. Xu).

https://doi.org/10.1016/j.ejrad.2019.07.021
Received 22 January 2019; Received in revised form 13 July 2019; Accepted 16 July 2019

imaging (DTI) can provide detailed information about brain white matter microstructure, such as fiber orientation, white matter integrity, and degree of myelination [9,10]. Moreover, susceptibility-weighted imaging (SWI) can show microscopic hemorrhage in neonatal brain [11], while arterial spin labeling (ASL) can provide information on cerebral perfusion [12]. These MR modalities have been studied in neonates. However, MRI modalities are not well studied for detecting changes in the internal environment in neonatal HIE. The internal environment and brain metabolism are altered during hypoxic-ischemia.

Amide proton transfer (APT) imaging is a chemical exchange saturation transfer-based molecular MRI approach that is capable of indirect measurement of pH levels and endogenous mobile proteins at the cellular and molecular levels [13]. Therefore, APT imaging is a potential modality for *in vivo* characterization of the internal environment during hypoxic-ischemic brain injury.

Although APT imaging studies have been performed in animal hypoxic-ischemia models [14,15], and a marked change in pH in lesions before and after ischemic insult was found, no discernible variation in amide content was found during a short period, but to the best of our knowledge, no study has been done in human neonatal. The purpose of this study was to investigate whether APT imaging can differentiate neonatal mild

HIE from normal age-matched infants, and to explore the changes in pH or protein concentration in neonatal mild HIE.

2. Subjects and methods

2.1. Subjects

This study was approved by the medical ethics review board, and written informed parental consent was obtained before scanning. A total of 30 full-term infants with HIE (16 males and 14 females; mean postnatal age 4.2 days, age range 2–7 days; mean gestational age 39.5 weeks, range 37–42 weeks; and mean birth weight 3296 g, range 2460–4540 g), were recruited from the Department of Pediatrics in Nanfang Hospital between May 2017 and January 2018. All cases had perinatal asphyxia, and were defined by the presence of at least three of the following criteria: (1) fetal heart rate abnormalities; (2) meconium staining of amniotic fluid; (3) delayed onset of respiration; (4) early postnatal blood pH level < 7.1; (5) Apgar score at 5 min of < 5; (6) multi-organ failure, followed by symptoms of encephalopathy [16]. Encephalopathy was independently graded by two neonatologists using Siben HIE scores [17]. HIE was classified as mild, moderate or severe, and each evaluated item varied according to the degree of severity, as previously described [17], if a slight change in the level of consciousness, a change in posture with mild distal flexion and weak suction are found in a newborn with a history of a hypoxic ischemic insult, we could classify this newborn as presenting mild HIE. Furthermore, all cases were diagnosed as mild HIE. Neonates with congenital malformations, trauma, central nervous system infections, and those born prior to reaching 36-week gestational age, were not included in the study. In all neonates, prescribed supportive treatment was immediately started after clinical diagnosis of HIE was established. None of mild HIE infants was treated with therapeutic hypothermia.

Twelve healthy neonates (six males and six females; mean postnatal age 3.3 days, age range 2–5 days; mean gestational age 39.5 weeks, range 37–42 weeks; and mean birth weight of 3136.67 g, range 2170–4000 g) with no evidence of birth asphyxia were recruited in the control group. In all neonates, conventional MRI and APT imaging were performed within 2–7 days after birth.

Neurodevelopmental assessment was done using a 20-item neonatal behavioral neurological assessment (NBNA) [18] at approximately 28 days of ages, administered by a trained pediatric developmental specialist with six years of experience, in conjunction with a neurodevelopmental pediatrician with > 10 years' experience.

2.2. MRI

During the MRI procedures, all neonates requiring sedation were sedated with oral chloral hydrate (10 mg/Kg), MR-compatible pulse oximetry and ECG data were monitored. Vacuum pillows were utilized to minimize subjects' movements during MRI. Ear protection from noise exposure was provided by earplugs and/or earmuffs. To ensure optimal monitoring and reduce the risk during transfer to the MRI room and MRI procedures, all investigations were performed under the supervision of a neonatologist.

MRI was performed on a 3 T MRI scanner (Achieva; Philips Healthcare, Best, the Netherlands), using a dual-channel body coil for transmission and an eight-channel sensitivity-encoding head coil for reception. Conventional MRI included axial T1-weighted (repetition time, 600 ms; echo time, 10 ms; slice thickness, 4 mm; no gap between slices), T2-weighted (repetition time, 3000 ms; echo time, 100 ms; slice thickness, 4 mm; no gap between slices), fluid-attenuated inversion recovery (FLAIR; repetition time, 9000 ms; echo time, 130 ms; inversion recovery time, 2300 ms; slice thickness, 4 mm; no gap between slices) and diffusion-weighted (repetition time, 3463 ms; echo time, 114.3 ms; b factors, 0 and 800 s/mm2; slice thickness, 4 mm; no gap between slices) images.

2.3. MRI scores

Neonatal brain injury on MRI (T1WI, T2WI, and DWI) was scored as previously described [1]. In the scoring system, five regions were qualitatively assessed including: (i) the subcortical region (caudate nucleus, globus pallidus/putamen, thalamus, and posterior limb of the internal capsule PLIC) (ii) white matter, (iii) cortex, (iv) cerebellum and (v) brainstem. Each subcortical component was independently scored. Each region was scored based on signal abnormality in each hemisphere on T1WI, T2WI and DWI. The brainstem was scored from 0 to 2 in all three sequences, because it is smaller than the other regions. A cumulative score was the summation of the five regional subscores, and classified as no (score: 0), mild (score: 1–11), moderate (score: 12–32), and severe injury (score: 33–138).

2.4. APT image acquisition

APT imaging was implemented using a fat-suppression, three-dimensional TSE-Dixon pulse sequence. The saturation pulse with a duration of 2 s (40 × 50 ms, sinc-Gauss-shaped elements) and power level of 2μT was obtained with two alternated RF transmission channels, which enable long RF irradiation. The saturation frequency offsets (± 3.5, ± 3.42, ± 3.58, −1540 ppm) were acquired via TSE-Dixon scanning with intrinsic B0 mapping and online reconstruction of B0-corrected APT images. B0 map was derived from three acquisitions at +3.5 ppm with different echo shifts. The remaining parameters were as follows: TR/TE = 6835/6,8 ms; FOV, 140 × 119 × 68 mm3; voxel size, 1.2 × 1.2 × 4 mm3; matrix, 116 × 99; SENSE factor, 2.25; scan duration, 5 min 20 s.

2.5. Selection of ROIs

Previous MRI studies have demonstrated the distribution and frequency of brain injury associated with neonatal HIE. The most common injury patterns involve either injury to the watershed region, or the deep grey nuclei consisting of the basal ganglia and thalamus [4]. Therefore, nine ROIs were selected including bilateral caudate, bilateral globus pallidus/putamen, bilateral thalamus, bilateral centrum semiovale, and brainstem (Fig. 1). The acquired APT images and all conventional MRI studies were evaluated by two blinded senior radiologists, and then quantified. ROIs were manually drawn on the APT images, avoiding interference of the skull, CSF, and cerebral ventricles. The APT value of the ROI indicated the signal intensity. MTR_{asym}

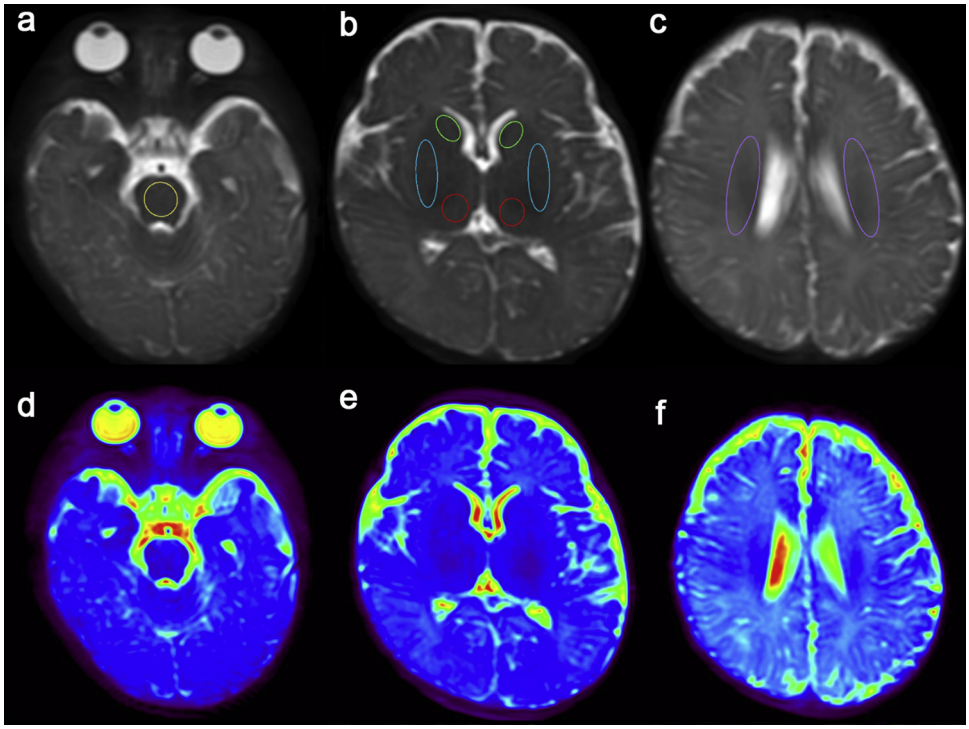

Fig. 1. ROIs selection. Images from T2WI (a–c) and APT sequences (d–f) are referenced for the selection of ROIs in this study. For all neonates, ROIs are chosen bilaterally in the caudate (green), the putamen (blue), the thalamus (red), the centrum semiovale (purple), and the brainstem (yellow).

analysis was employed for the calculation of APT values. The APT weighted images were calculated according to the equation:

$$MTRasym(\%) = (S - \Delta\omega - S\Delta\omega)/S0,$$

where $S-\Delta\omega$ is B0 corrected signal at -3.5 ppm, and $S\Delta\omega$ is B0 corrected signal at 3.5 ppm, and S0 is the normalization factor acquired at −1540ppm [19].

2.6. Statistical analysis

The statistical analysis was performed using SPSS version 13.0 statistical software for Windows (SPSS, Inc., Chicago, IL, USA). Data was presented as mean ± standard deviation. The difference in APT values between the mild HIE neonates and the control group was analyzed with the independent-samples t-test. The correlation between APT values and age-related changes for each region was analyzed by Pearson's correlation analysis. $P < 0.05$ indicated statistically significant difference.

3. Results

3.1. Clinical characteristics

All neurological examinations were performed by pediatricians. Study populations are comprised of 30 full-term neonates with mild HIE as cases and 12 full-term neonates as controls. All the 42 neonates had normal NBNA at approximately 28 days of ages. There was no statistical difference in gender, birth weight, gestation age, and postnatal age. Cord blood pH was significantly reduced and lactate was significantly increased in HIE as compared to the controls. Clinical characteristics of the study participants are summarized in Table 1.

3.2. MRI

By definition, the conventional MRIs were read by a senior radiologist in the control group no significant incidental or pathological findings were observed. Of the 30 mild HIE neonates, 10% (3/30) had a normal conventional MRI. MRI score was 5.67 ± 3.76 in the HIE group.

Individual APT values per region in all neonates were shown in Table 2. Fig. 2 and Table 3 exhibits the APT values of the control group and mild HIE group in all ROIs. APT values of the control group and the HIE group differed significantly in right caudate, right thalamus, left caudate, left globus pallidus/putamen, left thalamus, right centrum semiovale, and left centrum semiovale ($p < 0.05$). No statistical difference in APT values was observed in right globus pallidus/putamen ($p = 0.051$) and brainstem ($p = 0.073$) between the two groups.

Table 1
Baseline characteristics of the infants and Neurodevelopmental outcomes.

	Control group (N = 12)	Mild HIE group (N = 30)	statistics	P-value
Gender				
Male	6	16	$X^2 = 0.038$	0.845
Female	6	14		
Birth weight (g)	3136.67(476.28)	3296.00(464.93)	t = −0.997	0.325
GA at birth (weeks)	39.45(0.87)	39.52(1.20)	t = −0.185	0.854
GA at scan (weeks)	40.16(0.86)	40.13(1.31)	t = 0.055	0.957
Cord blood pH	7.34(0.10)	7.23(0.10)	t = 3.097	0.004*
Lactate	3.17(1.64)	5.73(2.42)	t = −3.351	0.002*
Apgar score	< 5 [n (%)]			
At 1 min	0(0)	1 (3%)		
At 5 min	0(0)	0(0)		
MR scores	0(0)	5.67(3.76)	t = 1.939	0.06
NBNA scores	39.17(0.83)	38.43(1.19)	t = 1.939	0.06

GA, gestational age; HIE, hypoxic-ischemic encephalopathy; NABA, neonatal behavioral neurological assessment.
Data are mean (standard deviation).
* < 0.05.

Table 2
Individual APT values per region in all neonates.

	Right Caudate	Right globus pallidus/Putamen	Right Thalamus	Left Caudate	Left globus pallidus/ Putamen	Left Thalamus	Brainstem	Right centrum semiovale	Left centrum semiovale
Control									
Subject 1	1.77	2.52	1.98	1.53	1.50	1.56	2.41	1.67	1.88
Subject 2	3.34	3.67	3.78	3.73	3.67	3.37	3.19	2.25	2.39
Subject 3	1.09	2.78	3.74	1.71	0.89	2.74	2.94	3.13	2.16
Subject 4	2.82	2.92	3.16	3.02	3.18	3.35	2.74	1.97	2.21
Subject 5	2.79	3.26	3.52	2.02	2.56	2.80	2.89	2.66	2.91
Subject 6	2.82	2.81	3.02	2.54	2.62	3.01	2.82	2.37	2.32
Subject 7	3.24	3.24	3.41	2.99	3.27	3.31	3.11	2.42	2.95
Subject 8	0.07	0.45	0.34	0.36	0.00	0.19	1.54	0.53	1.15
Subject 9	0.03	0.63	0.62	0.56	0.32	0.91	1.32	0.29	0.07
Subject 10	2.90	3.48	3.59	3.06	2.90	2.89	3.43	2.76	2.38
Subject 11	2.65	3.03	3.00	2.82	3.06	2.61	2.63	3.07	2.84
Subject 12	2.48	2.22	2.39	2.19	2.36	2.37	2.87	2.77	2.44
Mild HIE									
Subject 1	2.09	3.13	4.04	3.68	3.76	4.89	3.83	3.92	2.32
Subject 2	3.88	3.42	4.95	2.75	3.69	4.74	3.94	3.16	3.42
Subject 3	2.70	2.84	2.26	2.78	2.86	3.27	2.20	2.75	2.55
Subject 4	3.24	3.38	3.69	3.06	3.70	3.98	3.42	2.79	3.10
Subject 5	2.59	2.69	3.23	2.75	2.24	2.49	2.80	2.90	3.10
Subject 6	2.75	3.33	2.95	3.06	2.97	2.97	2.06	2.70	2.29
Subject 7	3.12	3.01	3.47	2.27	3.06	3.04	1.91	2.91	2.83
Subject 8	3.82	4.11	6.81	5.88	5.37	4.31	4.59	4.77	4.45
Subject 9	2.00	2.07	2.60	2.42	2.15	2.44	2.82	2.27	1.98
Subject 10	2.09	3.03	4.22	2.23	2.88	3.14	2.61	2.27	2.30
Subject 11	2.70	3.02	3.34	2.41	2.88	3.15	2.64	2.64	2.84
Subject 12	3.26	2.98	3.52	3.34	3.27	3.35	3.54	2.30	2.49
Subject 13	2.88	3.12	3.28	2.30	2.71	3.15	3.39	2.53	2.36
Subject 14	2.71	5.80	7.78	3.40	6.14	3.98	3.41	4.69	3.14
Subject 15	3.72	3.95	4.55	4.31	4.32	4.62	2.74	3.85	3.61
Subject 16	2.86	3.01	2.85	2.51	2.73	3.39	2.44	2.15	2.46
Subject 17	2.88	3.01	3.25	2.64	2.63	3.04	3.61	2.51	2.60
Subject 18	2.69	3.06	3.35	2.65	3.10	3.29	2.50	2.68	3.02
Subject 19	2.73	2.87	3.13	3.08	2.54	3.42	3.64	2.87	2.88
Subject 20	2.94	3.19	3.05	3.79	3.52	3.26	3.27	2.66	1.91
Subject 21	2.66	2.81	2.70	2.45	2.78	3.07	2.17	2.55	2.73
Subject 22	3.66	3.94	4.53	3.65	3.75	4.20	4.01	3.56	3.50
Subject 23	3.75	3.81	4.24	4.28	4.33	4.23	4.45	3.56	3.38
Subject 24	2.88	2.66	2.56	1.69	2.78	2.60	1.88	2.94	3.10
Subject 25	2.38	2.25	2.71	2.75	2.72	2.53	3.90	2.59	2.65
Subject 26	2.71	2.76	2.37	1.57	1.89	1.49	2.44	2.45	1.39
Subject 27	5.03	2.98	3.80	2.51	3.27	4.29	4.90	3.21	3.61
Subject 28	4.79	2.58	5.08	3.72	2.69	4.29	3.30	2.18	2.52
Subject 29	2.78	2.71	2.42	2.89	2.56	2.60	2.26	2.67	2.56
Subject 30	2.13	2.47	2.48	2.00	2.17	2.28	3.71	2.10	2.09

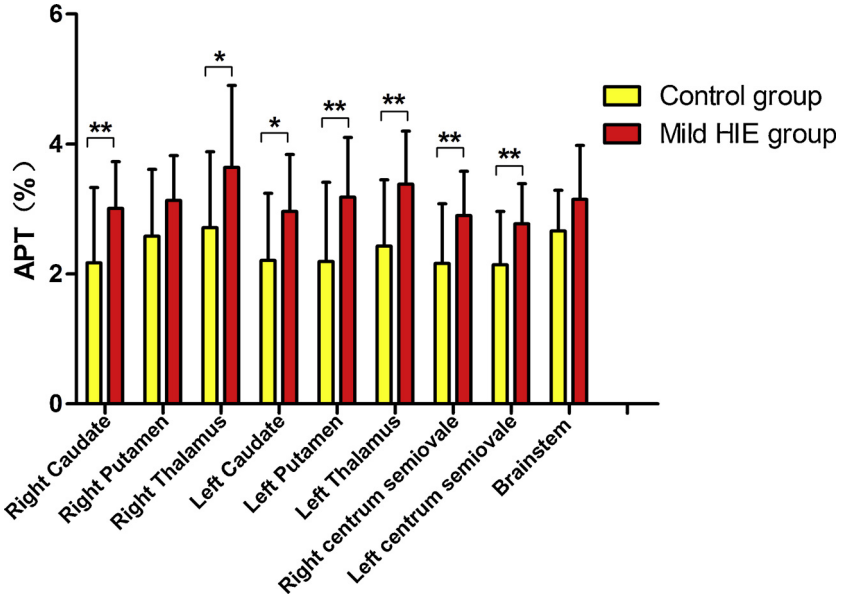

Fig. 2. Comparison of ROI-based APT values between healthy control group and neonates with mild HIE group. *p < 0.05; **p < 0.01.

Table 3
APT measurements at different ROIs.

ROIs	Control group (N = 12)	Mild HIE group(N = 30)	t-value	p-value
Right Caudate	2.17(1.16)	3.01(0.72)	−2.859	0.007*
Right globus pallidus/Putamen	2.58(1.03)	3.13(0.69)	−2.009	0.051
Right Thalamus	2.71(1.17)	3.64(1.26)	−2.194	0.034*
Left Caudate	2.21(1.03)	2.96(0.88)	−2.383	0.022*
Left globus pallidus/Putamen	2.19(1.22)	3.18(0.92)	−2.850	0.007*
Left Thalamus	2.43(1.02)	3.38(0.82)	−3.195	0.003*
Right centrum semiovale	2.16(0.92)	2.90(0.68)	−2.892	0.006*
Left centrum semiovale	2.14(0.82)	2.77(0.62)	−2.727	0.009*
Brainstem	2.66(0.63)	3.15(0.83)	−1.841	0.073

HIE, hypoxic-ischemic encephalopathy.
* < 0.05.

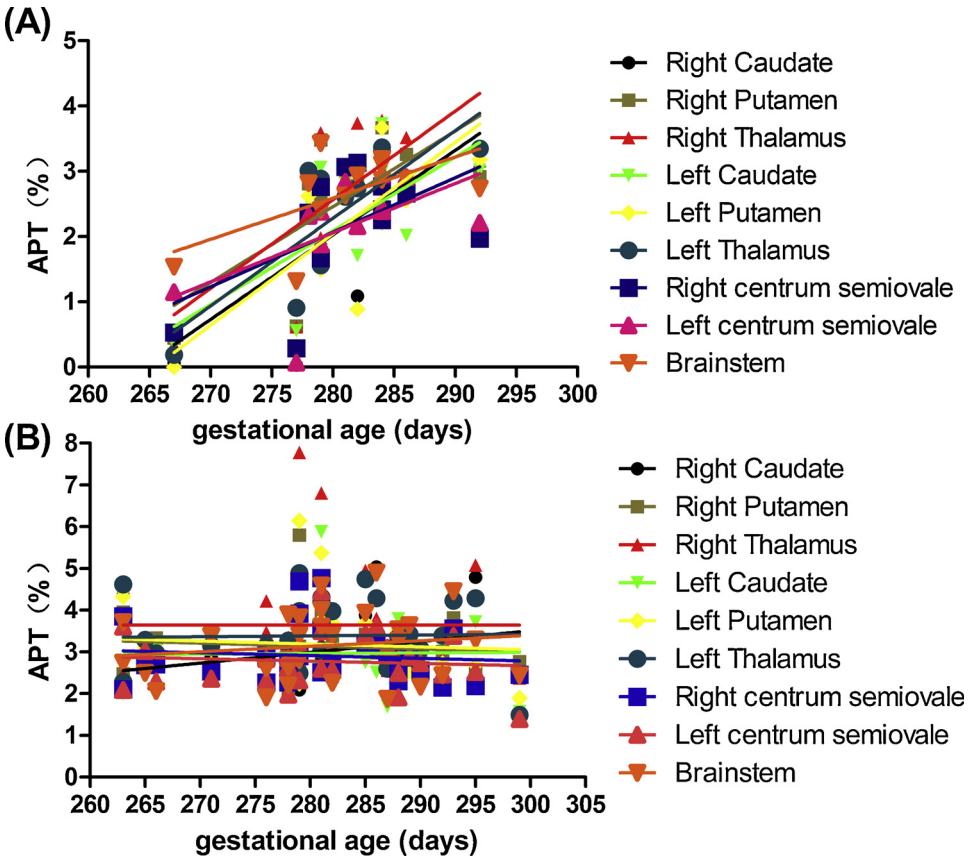

Fig. 3. Correlations between gestational age (days) and APT values in healthy control group (A), and mild HIE group (B). The black line, the darkKhaki line, the red line, the lime line, the yellow line, the darkcyan line, the blue line, the pink line, and the orange line reflect APT values in the right caudate, right putamen, right thalamus, left caudate, left putamen, left thalamus, right centrum semiovale, left centrum semiovale, and brainstem, respectively. R2 values in healthy control groups are as fllows: right caudate: 0.45, right putamen: 0.46, right thalamus: 0.49, left caudate: 0.43, left putamen: 0.48, left thalamus: 0.63, and brainstem: 0.36.

3.3. Correlation between APT values and age

The relation between APT values and age is shown in Fig. 3. Descriptive statistical outcomes are summarized in Table 4. In the control groups, the Pearson correlation coefficient between APT values and age showed positive correlation in most regions except for right (Pearson's r = 0.554, p = 0.062) and left centrum semiovale (Pearson's r = 0.561, p = 0.058). In the mild HIE groups, there was no significant correlation between APT values and gestational age in all regions.

4. Discussion

The neonatal brain development is a continuous process, with a large oxygen demand. Normally, energy required for brain activity is supported from the aerobic metabolism of glucose [20,21]. However, exposure to a hypoxic-ischemic environment alters the aerobic metabolism of carbohydrates in the brain. Whereby cellular metabolism uses anaerobic oxidation as opposed to the usual process of oxidative

Table 4
Pearson Correlations betweem gestation age (days) and APT values in different regions in two groups.

ROIs	Control group (N = 12)		Mild HIE group(N = 30)	
	R^2	P-value	R^2	P-value
Right caudate	0.673	0.016*	0.328	0.077
Right globus pallidus/putamen	0.680	0.015*	−0.090	0.637
Right thalamus	0.702	0.011*	0.002	0.992
Left caudate	0.664	0.019*	0.015	0.937
Left globus pallidus/putamen	0.695	0.012*	−0.068	0.720
Left thalamus	0.798	0.002*	0.023	0.903
Right centrum semiovale	0.554	0.062	−0.088	0.643
Left centrum semiovale	0.561	0.058	−0.083	0.662
Brainstem	0.604	0.037*	0.146	0.441

HIE, hypoxic-ischemic encephalopathy.
* < 0.05.

phosphorylation. In this case, energy is derived primarily from glycolysis. During glycolysis, lactate acid is produced, lactate accumulation further causes acidosis, thus suppressing glucose metabolism and consuming ATP, which aggravate intracellular acidosis [21,22].

APT imaging is a Chemical Exchange Saturation Transfer technique, which explores proteins and peptides containing protons that resonate at 3.5 ppm downfield from water. In theory, APT signal intensity primarily depends on the exchange rate between amide protons and water protons, and is associated with the protein content, pH, and temperature [14,23]. Therefore, APT imaging enhances the direct evaluation of molecular pathophysiological changes in the brain during hypoxia-ischemia. Zhou et al. [14,15] developed a mouse model of middle cerebral artery occlusion. They found a significant change in pH in lesions before and after ischemic insult, and a pH change of 0.5 units corresponded to a 50–70% change in the exchange rate. Thus, this finding supported the application of APT imaging in hypoxic-ischemic insult.

The present study showed that APT values were higher for neonates with mild HIE during days 3–7. In the hypoxic-ischemic brain injury animal model, APT signals initially decreased and reached the lowest level at 0–2 h, thereafter, the signals gradually increased, recovered to the level of the control group at 12–24 h, and then continued to increase. They were higher than the control group levels at 48–72 h [24]. The timing of hypoxic-ischemic brain injury is often difficult to accurately estimate. It is known that the majority of hypoxic-ischemic injuries occur intra-partum, while a minority occurs ante-partum and post-partum [4]. In the vast majority of infants with mild neonatal encephalopathy, the hypoxic-ischemic injury occurred during intra-partum [4]. Therefore, MRI of most neonates with mild HIE was initially conducted during hypoxemia and ischemia. Perhaps brain tissues undergo reperfusion after hypoxic-ischemia. Locally accumulated metabolites in brain tissue are excreted by reperfusion, and accompanied by the restoration of aerobic metabolism. Studies have also found that when brain tissue undergoes hypoxic-ischemia, pH transiently decreases and then increases, inducing rebound alkalosis [24]. This may be the reason for higher APT values in mild HIE in our study.

Ongoing brain development is also affected in neonates with HIE [25,26]. In the normal controls, we found that the APT values in most regions except for bilateral centrum semiovale exhibited a linear, positive correlation with gestational age. However, APT values were not significantly correlated with gestational age at all regions in the mild HIE group. The neonatal brain development is a dynamic process, which manifests as neuroglial cell proliferation and myelination [27]. Neuroglial cell proliferation is observed as an increase in cell density, and generally accompanied by the synthesis of numerous proteins for myelination [28–30]. Myelination is a process during which the oligodendroglial cell membrane curls and encloses nerve fibers to form the myelin sheath, and neuroglial cell proliferation is observed with the synthesis of several proteins [26,28,31]. Therefore, the process of myelination is associated with continuously increasing protein content during the course of brain development and maturation, which stabilizes in adulthood. Higher APT values reflect relatively higher semisolid macromolecular and protein contents. However, when energy metabolism is disrupted during the process of brain development in HIE, protein synthesis will be inevitably affected. Thus, the linear relationship between APT values and gestational age ceases to exist in neonates with HIE. Furthermore, APT measurements showed no significant differences in bilateral centrum semiovale (right: Pearson's $r = 0.554$, $p = 0.062$; left: Pearson's $r = 0.561$, $p = 0.058$) in this study. This may be partially limited by the smaller size of the control population. Theoretically, the small number of subjects could have fostered a slight bias in the measured correlation between APT values and different gestational ages [26].

In this study, the basal ganglia, thalamus, centrum semiovale, and brainstem were selected as ROIs for APT imaging. MRI studies have documented that the commonest brain injuries in neonatal encephalopathy involved either the watershed region, or the deep grey nuclei consisting of the basal ganglia and thalamus [4]. Watershed region injury is classically associated with sub-acute asphyxia, hypotension and impaired autoregulation [32,33]. It occurs in 40–60% of hypoxic-ischemic cases. Basal ganglia and thalamus injury is associated with acute severe asphyxia, and occurs in 40–80% of hypoxic-ischemic cases [32,33]. Furthermore, a less potentially catastrophic pattern of injury following severe asphyxia is associated with basal ganglia, thalamus and brainstem injury, occurring in 15–20% of cases [4]. Therefore, such an ROI can increase the sensitivity of biochemical tests.

Since the limited published data have focused on mild neonatal encephalopathy, it has been difficult to detail the true incidences of a MRI abnormality in hypoxic-ischemia. A recent study found that of 132 infants with mild neonatal encephalopathy, 59% (79/132) had an abnormal MRI in the Children's Hospital Neonatal Database [34]. In our study, we found that three infants with mild neonatal encephalopathy had a normal conventional MRI. Therefore, some infants with mild HIE cannot be detected with conventional MRI in the neonatal stage. However, APT imaging can play a complementary role in detecting patients with mild HIE.

There were several limitations to this study. Firstly, APT imaging is highly sensitive to changes in protein contents and pH values. We did not measure the pH values in the brain tissues. The brain internal environment is also somewhat complicated. Therefore, simple APT imaging analysis cannot distinguish between pH effects and protein information. Secondly, myelination during brain development will have varying influence on the APT values in the neonatal brain. Thus, APT imaging of HIE should be evaluated based on neonate gestational age [26]. Thirdly, the small sample size may have restricted our power to detect the relationship between APT values and different gestational ages. Finally, APT imaging is technically limited by a low signal-to noise ratio, so it is not widely used to assess the intracellular environment. Therefore, it is necessary to optimize scan sequence parameters [13,35], reduce artifacts, and develop new imaging algorithms [14,36] in the application of APT imaging.

5. Conclusions

In summary, our study indicated that APT imaging for neonatal mild HIE is a useful and feasible technique with diagnostic capability. APT imaging offers effective new tools for the characterization of brain internal environment that could enhance our understanding of the pathogenesis of neonatal HIE.

Declaration of competing interest

All authors have no conflict of interest to report.

Consent for publication

Yes, all authors consent to publish this manuscript.

Funding

This work was supported by the China-American Construction of Center for Transformational Medicine for Developmental Defects [Grant number 2015B050501006]; National Key Research and Development Program of China [Grant number 2016YFC0107104]; Science and Technology Planning Project of Guangdong Province, China [Grant number 2015B010131011].

Authors' contributions

Yikai Xu and Mei Zhong conceived and designed the study. Sijin Chen, Xilong Liu, Yingjie Mei, Caixia Li and Daokun Ren performed the experiments. Sijin Chen and Xilong Liu wrote the paper. Yingjie Mei,

Yikai Xu and Mei Zhong reviewed and edited the manuscript. All authors read and approved the manuscript.

Acknowledgements

This work was partly funded by the China-American Construction of Center for Transformational Medicine for Developmental Defects [Grant number 2015B050501006]; the National Key Research and Development Program of China [Grant number 2016YFC0107104] and the Science and Technology Planning Project of Guangdong Province, China [Grant number 2015B010131011]. The authors express their appreciation to their patients and volunteers for participating in this study.

References

[1] S.B. Trivedi, Z.A. Vesoulis, R. Rao, et al., A validated clinical MRI injury scoring system in neonatal hypoxic-ischemic encephalopathy, Pediatr. Radiol. 47 (11) (2017) 1491–1499.
[2] V. Chau, K.J. Poskitt, C.P. Dunham, G. Hendson, S.P. Miller, Magnetic resonance imaging in the encephalopathic term newborn, Curr. Pediatr. Rev. 10 (1) (2014) 28–36.
[3] M.E. Dilenge, A. Majnemer, M.I. Shevell, Long-term developmental outcome of asphyxiated term neonates, J. Child Neurol. 16 (11) (2001) 781–792.
[4] B.H. Walsh, T.E. Inder, MRI as a biomarker for mild neonatal encephalopathy, Early Hum. Dev. 120 (2018) 75–79.
[5] J.M. Conway, B.H. Walsh, G.B. Boylan, D.M. Murray, Mild hypoxic ischaemic encephalopathy and long term neurodevelopmental outcome — a systematic review, Early Hum. Dev. 120 (2018) 80–87.
[6] Y.K. Lee, A. Penn, M. Patel, R. Pandit, D. Song, B.Y. Ha, Hypothermia-treated neonates with hypoxic-ischemic encephalopathy: optimal timing of quantitative ADC measurement to predict disease severity, Neuroradiol. J. 30 (1) (2017) 28–35.
[7] G.K. Malik, M. Pandey, R. Kumar, S. Chawla, B. Rathi, R.K. Gupta, MR imaging and in vivo proton spectroscopy of the brain in neonates with hypoxic ischemic encephalopathy, Eur. J. Radiol. 43 (1) (2002) 6–13.
[8] J.L. Wisnowski, T.W. Wu, A.J. Reitman, et al., The effects of therapeutic hypothermia on cerebral metabolism in neonates with hypoxic-ischemic encephalopathy: an in vivo 1H-MR spectroscopy study, J. Cereb. Blood Flow Metab. 36 (6) (2016) 1075–1086.
[9] M.E. Lemmon, M.W. Wagner, T. Bosemani, et al., Diffusion tensor imaging detects occult cerebellar injury in severe neonatal hypoxic-ischemic encephalopathy, Dev. Neurosci. 39 (1–4) (2017) 207–214.
[10] Y. Seo, G.T. Kim, J.W. Choi, Early detection of neonatal hypoxic-ischemic white matter injury: an MR diffusion tensor imaging study, Neuroreport 28 (13) (2017) 845–855.
[11] D. Tortora, M. Severino, M. Malova, A. Parodi, G. Morana, L.A. Ramenghi, A. Rossi, Variability of cerebral deep venous system in preterm and term neonates evaluated on MR SWI venography, AJNR Am. J. Neuroradiol. 37 (11) (2016) 2144–2149.
[12] J.B. De Vis, J. Hendrikse, E.T. Petersen, et al., Arterial spin-labelling perfusion MRI and outcome in neonates with hypoxic-ischemic encephalopathy, Eur. Radiol. 25 (1) (2015) 113–121.
[13] Y. Zheng, X. Wang, The applicability of amide proton transfer imaging in the nervous system: focus on hypoxic-ischemic encephalopathy in the neonate, Cell. Mol. Neurobiol. 38 (4) (2018) 797–807.
[14] J. Zhou, J.F. Payen, D.A. Wilson, R.J. Traystman, P.C. van Zijl, Using the amide proton signals of intracellular proteins and peptides to detect pH effects in MRI, Nat. Med. 9 (8) (2003) 1085–1090.
[15] P.Z. Sun, J. Zhou, W. Sun, J. Huang, P.C. van Zijl, Detection of the ischemic penumbra using pH-weighted MRI, J. Cereb. Blood Flow Metab. 27 (6) (2007) 1129–1136.
[16] L. Guo, D. Wang, G. Bo, H. Zhang, W. Tao, Y. Shi, Early identification of hypoxic-ischemic encephalopathy by combination of magnetic resonance (MR) imaging and proton MR spectroscopy, Exp. Ther. Med. 12 (5) (2016) 2835–2842.
[17] J.M. Perez, S.G. Golombek, A. Sola, Clinical hypoxic-ischemic encephalopathy score of the Iberoamerican Society of Neonatology (Siben): a new proposal for diagnosis and management, Rev. Assoc. Med. Bras. (1992) 63 (1) (2017) 64–69.
[18] X.L. Bao, R.J. Yu, Z.S. Li, 20-item neonatal behavioral neurological assessment used in predicting prognosis of asphyxiated newborn, Chin. Med. J. 106 (3) (1993) 211.
[19] V. Guivel-Scharen, T. Sinnwell, S.D. Wolff, R.S. Balaban, Detection of proton chemical exchange between metabolites and water in biological tissues, J. Magn. Reson. (San Diego, Calif: 1997) 133 (1) (1998) 36–45.
[20] E.J. Dickey, S.N. Long, R.W. Hunt, Hypoxic ischemic encephalopathy—what can we learn from humans? J. Vet. Intern. Med. 25 (6) (2011) 1231–1240.
[21] M.C. Lai, S.N. Yang, Perinatal hypoxic-ischemic encephalopathy, J. Biomed. Biotechnol. 2011 (2011) 609813.
[22] G. Distefano, A.D. Pratico, Actualities on molecular pathogenesis and repairing processes of cerebral damage in perinatal hypoxic-ischemic encephalopathy, Ital. J. Pediatr. 36 (2010) 63.
[23] K.T. Jokivarsi, H.I. Grohn, O.H. Grohn, R.A. Kauppinen, Proton transfer ratio, lactate, and intracellular pH in acute cerebral ischemia, Magn. Reson. Med. 57 (4) (2007) 647–653.
[24] Y. Zheng, X.M. Wang, Measurement of lactate content and amide proton transfer values in the basal ganglia of a neonatal piglet hypoxic-ischemic brain injury model using MRI, AJNR Am. J. Neuroradiol. 38 (4) (2017) 827–834.
[25] H. Zhang, H. Kang, X. Zhao, et al., Amide Proton Transfer (APT) MR imaging and Magnetization Transfer (MT) MR imaging of pediatric brain development, Eur. Radiol. 26 (10) (2016) 3368–3376.
[26] Y. Zheng, X. Wang, Magnetization transfer and amide proton transfer MRI of neonatal brain development, Biomed Res. Int. 2016 (2016) 3052723.
[27] N. Camargo, A. Goudriaan, A.F. van Deijk, et al., Oligodendroglial myelination requires astrocyte-derived lipids, PLoS Biol. 15 (5) (2017) e1002605.
[28] M. Bradl, H. Lassmann, Oligodendrocytes: biology and pathology, Acta Neuropathol. 119 (1) (2010) 37–53.
[29] N. Baumann, D. Pham-Dinh, Biology of oligodendrocyte and myelin in the mammalian central nervous system, Physiol. Rev. 81 (2) (2001) 871–927.
[30] M.A. van Buchem, S.C. Steens, H.A. Vrooman, et al., Global estimation of myelination in the developing brain on the basis of magnetization transfer imaging: a preliminary study, AJNR Am. J. Neuroradiol. 22 (4) (2001) 762–766.
[31] N. Girard, C. Raybaud, P. du Lac, MRI study of brain myelination, J. Neuroradiol. 18 (4) (1991) 291–307.
[32] L.T. Sie, M.S. van der Knaap, J. Oosting, L.S. de Vries, H.N. Lafeber, J. Valk, MR patterns of hypoxic-ischemic brain damage after prenatal, perinatal or postnatal asphyxia, Neuropediatrics 31 (3) (2000) 128–136.
[33] A.J. Barkovich, B.L. Hajnal, D. Vigneron, et al., Prediction of neuromotor outcome in perinatal asphyxia: evaluation of MR scoring systems, AJNR Am. J. Neuroradiol. 19 (1) (1998) 143–149.
[34] A.N. Massaro, K. Murthy, I. Zaniletti, et al., Short-term outcomes after perinatal hypoxic ischemic encephalopathy: a report from the Children's Hospitals Neonatal Consortium HIE focus group, J. Perinatol. 35 (4) (2015) 290–296.
[35] X. Zhao, Z. Wen, G. Zhang, et al., Three-dimensional turbo-spin-echo amide proton transfer MR imaging at 3-Tesla and its application to high-grade human brain tumors, Mol. Imaging Biol. 15 (1) (2013) 114–122.
[36] I.Y. Zhou, E. Wang, J.S. Cheung, X. Zhang, G. Fulci, P.Z. Sun, Quantitative chemical exchange saturation transfer (CEST) MRI of glioma using Image Downsampling Expedited Adaptive Least-squares (IDEAL) fitting, Sci. Rep. 7 (1) (2017) 84.